

# Design and Performance Analysis of a 420nm Oxide Confined MQW Blue-Violet Laser

**Nadia Afroze\*, Rinku Basak**

Department of Electrical and Electronic Engineering, American International University-Bangladesh (AIUB), Banani, Dhaka-1213, Bangladesh.

\*Correspondence: Email: [afrozenadia60@gmail.com](mailto:afrozenadia60@gmail.com), [nadiaafroze@aiub.edu](mailto:nadiaafroze@aiub.edu)

**Abstract:** In this work, the performance characteristics of an InGaN-based 420nm oxide confined multiple quantum well (MQW) blue-violet laser has been evaluated through various computations. Also the difference between the performance analysis of the designed laser with oxide confinement layer and without oxide confinement layer has been observed. The material gain of  $\text{In}_{0.1227}\text{Ga}_{0.8773}\text{N}/\text{Al}_{0.08}\text{Ga}_{0.92}\text{N}$  MQW edge emitting laser (EEL) has been theoretically obtained. The peak material gain obtained from the analysis has been used to study the performance of the designed laser. The threshold current has been reduced from 10.2mA to 3.4mA by using the oxide confinement layer. The injection current which is almost 13 times the threshold current has been chosen for both the designed laser with and without oxide confinement layer. The resonant frequency is 16.2GHz and modulation bandwidth 28.2GHz for the designed laser without oxide confinement layer at an injection current 130mA. The same value of resonant frequency and modulation bandwidth has been achieved for the designed laser with oxide confinement layer at an injection current of only 45mA. The maximum output power of the designed oxide confined laser is obtained as 73.4mW. The designed laser with oxide confinement layer has been established to give better performance.

**Keywords:** Blue-Violet Laser, Resonance Frequency, Modulation Bandwidth, Threshold Current, Oxide Confinement Layer.

## 1 INTRODUCTION

Semiconductor laser diodes with blue beams are typically based on gallium (III) nitride (GaN, violet color) or indium gallium nitride (often true blue in color, but also able to produce other colors). Both blue and violet lasers can also be constructed using frequency-doubling of infrared laser wavelengths from diode lasers or diode-pumped lasers.

Semiconductor laser diodes have applications in the field of optoelectronic data storage, printing, high density medical applications, spectroscopy etc. due to their small size, low power dissipation and high quantum efficiency. The laser diode can be designed for different emission wavelengths based on applications. Different types of low cost full color projection systems and high resolution laser color printers could be designed by moving towards shorter wavelength semiconductor laser diodes. The density and at the same time resolution can be enhanced by a diminution in emission wavelength of the semiconductor laser diode. Infra-red semiconductor laser diodes which are being reasonable prices are being broadly used.

Indium gallium nitride ( $\text{InGaN}$ ,  $\text{In}_x\text{Ga}_{1-x}\text{N}$ ) is a semiconductor material made of a mix of gallium nitride (GaN) and indium nitride (InN). It is a ternary group III/group V direct band gap semiconductor. The indium-rich regions have a lower band gap than the surrounding material and create regions of reduced potential energy for charge carriers. Its band gap can

be tuned by varying the amount of indium in the alloy. The ratio of In/Ga is usually between 0.02/0.98 and 0.3/0.7 (Aldrige *et al.* 2011). GaN is a defect-rich material with typical dislocation densities exceeding  $10^8 \text{ cm}^{-2}$  (Choi *et al.* 2004). Light emission from InGaN layers grown on such GaN buffers used in blue and green laser diodes (Eliseev 1999). InGaN quantum wells are efficient light emitters in green, blue, white and ultraviolet light-emitting diodes and diode lasers (Chen *et al.* 2010), (Chang *et al.* 2007), (Skierbiszewski *et al.* 2005).

The best semiconductor for blue-violet lasers is gallium nitride (GaN) crystals, which are much harder to manufacture, requiring higher pressures and temperatures. The active layer of the Nichia devices was formed from InGaN quantum wells. The new invention enabled the development of small, convenient and low-priced blue-violet, ultraviolet UV lasers and opened the way for applications such as high-density HD DVD data storage and Blue-ray discs. The shorter wavelength allows it to read discs containing much more information (Bergh 2004).

In this work, the difference between the performance characteristics of a 420nm designed laser with oxide confinement layer and without oxide confinement layer is presented with the aim of obtaining high performance characteristics for the designed oxide confined laser.

## 2 DEVICE STRUCTURE

In this work, an EEL whose active region contains three QWs of  $\text{In}_{0.1227}\text{Ga}_{0.8773}\text{N}$ , separated by  $\text{Al}_{0.08}\text{Ga}_{0.92}\text{N}$  barriers are chosen for simulation with a view to obtain 420nm operation. The cavity of the EEL consisting of two cladding layers of  $\text{Al}_{0.16}\text{Ga}_{0.84}\text{N}$ . The cladding and active layer materials are separated by two separate confinement heterostructure (SCH) layers of  $\text{Al}_{0.08}\text{Ga}_{0.92}\text{N}$ .

For achieving high performance, the In, Ga and N concentrations of the InGaN QW material is chosen by computing the concentration values using Vegard's law (Coldren *et al.* 1995). Values of a required number of parameters are obtained from different published sources (Piprek *et al.* 2000).

The band gap energy of InGaN is given by-

$$E_g(\text{In}_x\text{Ga}_{1-x}\text{N}) [eV] = E_g(\text{InN})x + E_g(\text{GaN})(1-x) - bx(1-x) \quad (1)$$

where  $b$  is the bowing parameter.

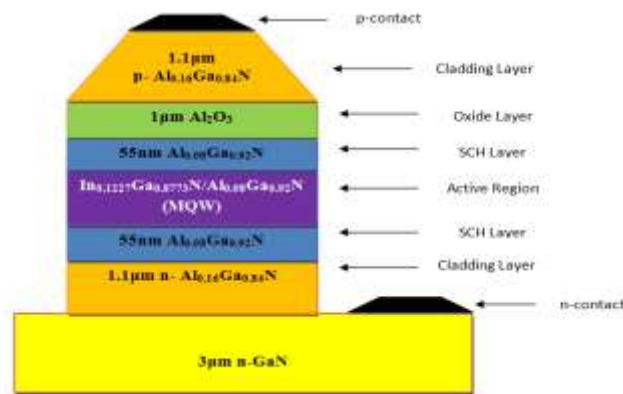


Fig. 1: The designed structure of a 420nm  $\text{In}_{0.1227}\text{Ga}_{0.8773}\text{N}/\text{Al}_{0.08}\text{Ga}_{0.92}\text{N}$  MQW Oxide Confined Blue-Violet Laser

The structure of a blue-violet laser, presented in Figure 1, consists of active region, barriers, SCH layers and oxide confinement layers. The active region of a blue-violet laser contains 3 QWs of  $\text{In}_{0.1227}\text{Ga}_{0.8773}\text{N}$  (band gap energy,  $E_{\text{gw}}=2.8232\text{eV}$ ; refractive index,  $n=2.6183$ ) of 5nm each and 2 barriers of  $\text{Al}_{0.08}\text{Ga}_{0.92}\text{N}$  (band gap energy,  $E_{\text{gb}}=3.5767\text{eV}$ ; refractive index,  $n=2.4723$ ) of 7nm each. The electron effective mass ( $m_e$ ) is  $0.18443m_0$  and the hole effective mass ( $m_h$ ) is  $0.29356m_0$  of the QW material, where  $m_0$  is the mass of electron. The total thickness of the active region is 29nm considering 3 QWs and 2 barriers; the width is  $2\mu\text{m}$  (without oxide confinement layer) and the length is  $780\mu\text{m}$ .

The active region of the laser is sandwiched by two separate confinement heterostructure (SCH) layers of  $\text{Al}_{0.08}\text{Ga}_{0.92}\text{N}$  ( $E_{\text{gb}}=3.5767\text{eV}$ ,  $n=2.4723$ ) of 55nm each. The total thickness of the cavity including SCH is calculated as 139nm. After adding the  $1\mu\text{m}$  oxide confinement layer of  $\text{Al}_2\text{O}_3$ , the new width of the active region is  $0.67\mu\text{m}$ . The p-type and n-type cladding layers of  $\text{Al}_{0.16}\text{Ga}_{0.84}\text{N}$  ( $E_{\text{gclad}}=3.7458\text{eV}$ ,  $n=2.4379$ ) are of  $1.1\mu\text{m}$  each. The confinement factor is calculated as  $\Gamma=0.2086$ . The n-GaN substrate of  $3\mu\text{m}$  is connected with the lower n-contact and the upper p-contact is connected with the p-cladding layer as shown in Figure 1.

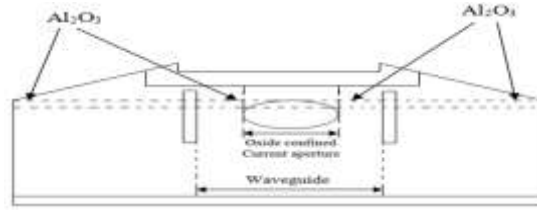


Fig. 2: Cross Sectional View of a 420nm  $\text{In}_{0.1227}\text{Ga}_{0.8773}\text{N}/\text{Al}_{0.08}\text{Ga}_{0.92}\text{N}$  MQW Oxide Confined Blue-Violet Laser

Figure 2 shows the cross-sectional view of the designed oxide-confined layer. The procedure of oxide confinement considered in this work is based on other research work (Erwin *et al.* 2005). To use the oxide confinement layer, the width has been reduced from  $2\mu\text{m}$  to  $0.67\mu\text{m}$ . As a result the active volume of the active region reduces from  $4.524 \times 10^{-11} \text{ cm}^3$  to  $1.51554 \times 10^{-11} \text{ cm}^3$  and the threshold current reduces from 10.2mA to 3.4mA.

### 3 SIMULATION RESULTS AND DISCUSSIONS

#### 3.1 Computation of Transparency Carrier Density $N_{tr}$ , Threshold Carrier Density $N_{th}$ , Photon Life Time $\tau_p$ and Threshold Current $I_{th}$ of the Designed Laser

The transparency carrier density of a material is related to the effective masses of carriers in the conduction band (CB) and valance band (VB) as (Coldren *et al.* 1995), (Basak 2013), (Alam *et al.* 2013)

$$N_{tr} = 2 \left( \frac{kT}{2\pi\hbar^2} \right)^{\frac{3}{2}} (m_c m_v)^{\frac{3}{4}} \quad (2)$$

where  $k$  is the Boltzmann constant,  $T$  is the temperature in K,  $\hbar$  is the Plank's constant divided by  $2\pi$ ,  $m_c$  and  $m_v$  are the effective masses of the carrier in the CB and VB, respectively. The relationship is used to compute the transparency carrier density of the QW material. At 300K, the calculated value of transparency carrier density for  $\text{In}_{0.1227}\text{Ga}_{0.8773}\text{N}$  is  $2.8 \times 10^{18} \text{ cm}^{-3}$ . This

value is lower than that of the barrier material for which it is suitable to be used as the QW material.

The threshold carrier density can be found using the following expression (Coldren *et al.* 1995)

$$N_{th} = N_{tr} e^{\frac{\langle \alpha_i \rangle + \alpha_m}{\Gamma g_o}} \quad (3)$$

where  $g_o$  is the material gain constant.

Using the obtained threshold carrier density, the photon lifetime is then calculated using the following expression (Coldren *et al.* 1995)

$$\tau_p = \frac{1}{v_g(\langle \alpha_i \rangle + \alpha_m)} \quad (4)$$

The photon life, from the above expression is 4.3269ps with a group velocity  $v_g$  of  $1.1786 \times 10^{10} \text{cms}^{-1}$ . The threshold current is then calculated using (Coldren *et al.* 1995)

$$I_{th} = \frac{qV_a N_{th}}{\eta_i \tau_c} \quad (5)$$

It is found that at 300K the threshold current is as small as 3.4mA with an injection current efficiency ( $\eta_i$ ) of 0.8.

### 3.2 Calculation of material gain

For designing an EEL structure the material gain is calculated as (Coldren *et al.* 1995) (Basak 2013), (Alam *et al.* 2013)

$$g(E) = \left( \frac{q^2 \pi \hbar}{\epsilon_o m_o^2 n c E} \right) |M_T|^2 \rho_r (f_2 - f_1) \quad (6)$$

where,  $q$  is the electron charge,  $\epsilon_o$  is the free-space permittivity,  $c$  is the speed of light in vacuum,  $n$  is the refractive index of the laser structure,  $E$  is the transition energy,  $n$  is the refractive index of the laser structure,  $|M_T|^2$  is the transition momentum matrix element,  $\rho_r$  is the reduced density of state,  $\hbar$  is the Planck's constant divided by  $2\pi$ ,  $f_2$  and  $f_1$  are the electron quasi-Fermi functions in the conduction and valence band respectively.

Using Eq. (6), the material gain for a 420nm  $\text{In}_{0.1227}\text{Ga}_{0.8773}\text{N}/\text{Al}_{0.16}\text{Ga}_{0.84}\text{N}$  MQW EEL is calculated at 300K by varying the wavelength. It is essential to arrange the band gap energy in such a way that the cavity oscillation occurs at the peak value of the gain of the material. The obtained results are plotted as shown in Figure 4. A peak material gain value of  $1101 \text{cm}^{-1}$  is obtained for  $\text{In}_{0.1227}\text{Ga}_{0.8773}\text{N}/\text{Al}_{0.08}\text{Ga}_{0.92}\text{N}$  MQW EEL around the lasing wavelength of 427.9nm.

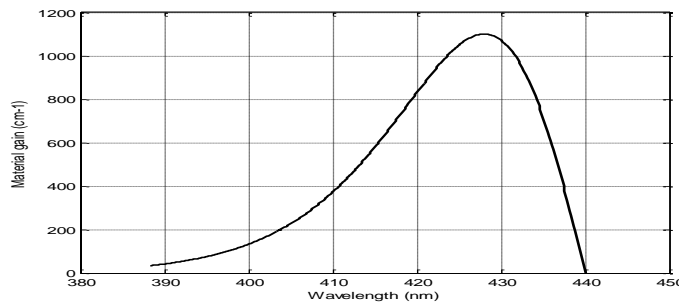


Fig. 3: Plot of Material gain Versus Wavelength of the designed  $\text{In}_{0.1227}\text{Ga}_{0.8773}\text{N}/\text{Al}_{0.08}\text{Ga}_{0.92}\text{N}$  3QW EEL at 300K. The material Gain of the Designed Laser Varies with the Variation of Wavelength and a maximum gain is obtained as  $1101\text{cm}^{-1}$  at  $427.9\text{nm}$  wavelength.

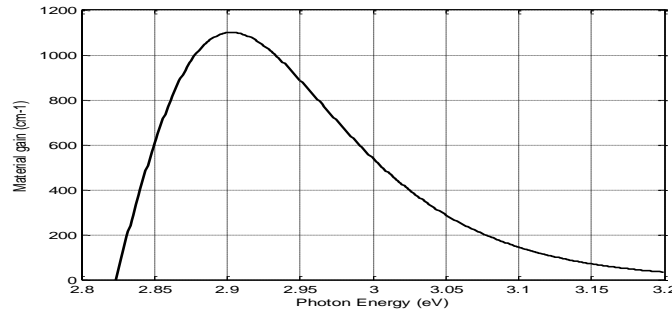


Fig. 4: Plot of Material gain Versus Photon energy of the designed  $\text{In}_{0.1227}\text{Ga}_{0.8773}\text{N}/\text{Al}_{0.08}\text{Ga}_{0.92}\text{N}$  3QW EEL at 300K. The material Gain of the Designed Laser Varies with the Variation of Photon energy and a maximum gain is obtained as  $1101\text{cm}^{-1}$  at  $2.902\text{eV}$ .

It is observed that at  $2.8232\text{eV}$  the material gain goes to positive level and a maximum gain is obtained as  $1101\text{cm}^{-1}$  at  $2.902\text{eV}$ . Using the obtained value of peak material, the gain of the performance analysis of the designed  $420\text{nm}$  EEL has been presented in the above section.

**3.3 Calculation of Carrier Density, Photon Density and Output Power**

The rate equations of a semiconductor laser are (Coldren *et al.* 1995)

$$\frac{dN}{dt} = \frac{\eta_i I}{qV_a} - \frac{N}{\tau_c} - \frac{v_g a(N - N_{tr})S}{1 + \epsilon S} \tag{7}$$

and,

$$\frac{dS}{dt} = \frac{\Gamma v_g a(N - N_{tr})S}{1 + \epsilon S} + \Gamma \beta_{sp} \frac{\eta_i I_{th}}{q} - \frac{S}{\tau_p} \tag{8}$$

A plot of carrier density versus time is shown in Figure 5 for both the designs of the laser, that is, with and without oxide confinement layer.

The solution of these rate equations have been obtained using the parameter values, for a time window of 0-3ns approximately using finite difference method in MATLAB for chosen value of injection current of  $45\text{mA}$  for the designed oxide confined  $420\text{nm}$  laser.

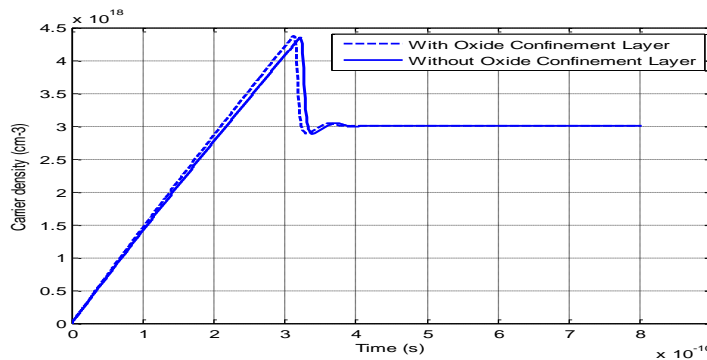


Fig. 5: Plots of Carrier Density versus Time for the Designed 420nm Laser both with and without oxide confinement layer.

The value of injection current is to be considered such that it is above threshold current. From Figure 5 the steady state carrier density is  $3.008 \times 10^{18} \text{ cm}^{-3}$  for the designed laser without oxide confinement layer at injection current 130mA. It is possible to reach the same value of steady state carrier density for the designed laser with oxide confinement layer only at an injection current 45mA.

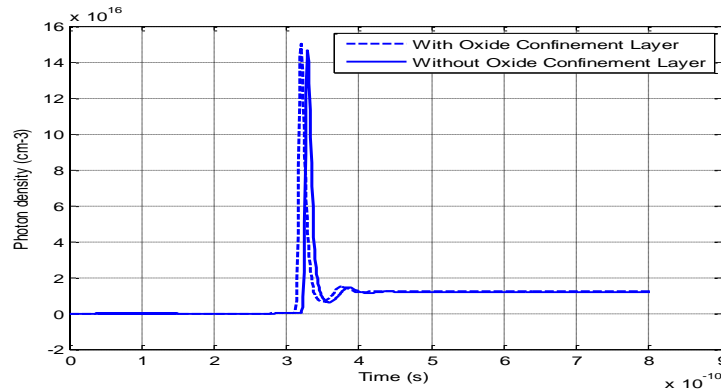


Fig. 6: Plots of Photon Density versus Time for the Designed 420nm Laser both with and without oxide confinement layer.

Using the output of the computational work above, a plot of photon density versus time is presented in Figure 6 for both the designs of the laser, that is, with and without oxide confinement layer.

From Figure 6 the steady state photon density is  $1.197 \times 10^{16} \text{ cm}^{-3}$  for the designed laser without oxide confinement layer at an injection current 130mA. The same value of steady state photon density has been obtained for the designed laser with oxide confinement layer only at an injection current 45mA.

With the aid of the varying nature of the photon density simulation, variation of output power can also be obtained from (Coldren *et al.* 1995)

$$P_{out} = v_g \alpha_m h \nu S V_p \tag{9}$$

Using Eq. (9) the steady state output power of the designed oxide confined laser is obtained as 73.4mW.

The output power of the designed laser can also be expressed in terms of material gain  $g$ , mirror loss coefficient  $\alpha_m$ , injection current  $I$  and threshold current  $I_{th}$  as(Coldren *et al.* 1995)

$$P_{out} = \frac{\alpha_m h \nu \eta_i}{q g \Gamma} (I - I_{th}) \tag{10}$$

Using, the output power of Eq. (10) and the parameter values presented above, plots of output power versus injection current for the designed 420nm laser both with and without oxide confinement layer are presented in Figure 7 after computations.

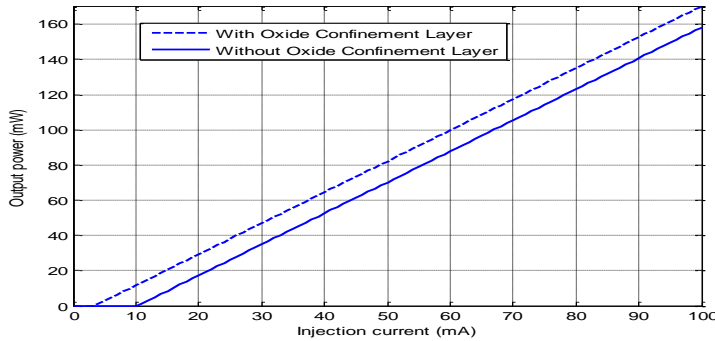


Fig. 7: Plots of Output Power versus Injection Current for the Designed 420nm Laser both with and without oxide confinement layer. A lower value of threshold current is obtained for the designed oxide-confined Laser.

From Figure 7 it is found that the threshold current for the designed laser without oxide confinement layer is 10.2mA and is 3.4mA with oxide confinement. After the threshold the output power increases with the increase of injection current.

The plot of output power versus wavelength is shown in Figure 8 for the designed oxide confined laser.

From Figure 8 it is observed that the output power has its peak value 31.5dBm at 420nm, which is the wavelength of the designed oxide confined laser.

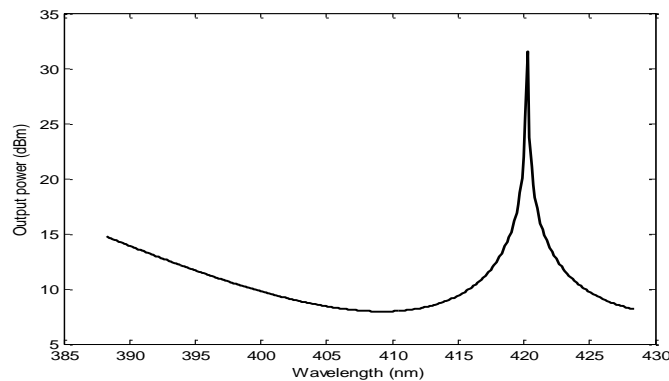


Fig. 8: Plot of Output Power versus Wavelength of the Designed Oxide Confined Laser at 300K, where injection current is 45mA. A Peak Intensity of the Power is obtained at 420nm Wavelength.

### 3.4 Calculation of modal gain

The confinement of material gain is called the modal gain and it is related to the carrier density as (Coldren *et al.* 1995)

$$\Gamma g = \Gamma g_o \ln \left( \frac{N}{N_{tr}} \right) \tag{11}$$

where  $\Gamma$  is the confinement factor,  $g_o$  is the material gain constant,  $N$  is carrier density, and  $N_{tr}$  is the transparency carrier density of QW material.

The plot of modal gain versus time is shown in Figure 9 for both the designs of the laser, that is, with and without oxide confinement layer.

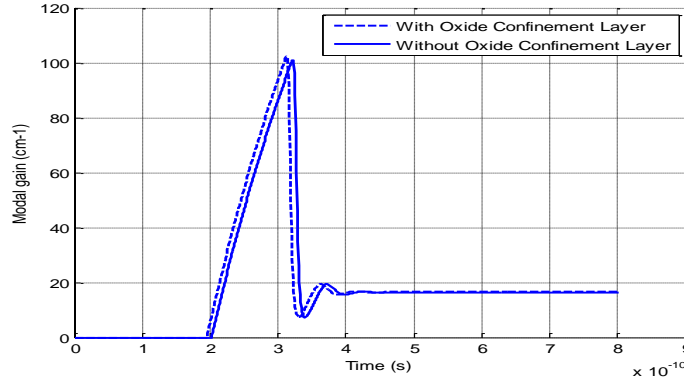


Fig. 9: Plots of Modal Gain versus Time for the Designed 420nm Laser both with and without oxide confinement layer.

From Figure 9 the steady state modal gain is  $16.4\text{cm}^{-1}$  for the designed laser without oxide confinement layer at an injection current 130mA. The same value of steady state modal gain has been achieved for the designed laser with oxide confinement layer only at an injection current of 45mA.

### 3.5 Modulation Response of the Designed Laser

The modulation response of the designed laser has been obtained using the equation of the transfer function as given below (Coldren *et al.* 1995) (Basak 2013)

$$H(f) = \frac{f_R^2}{f_R^2 - f^2 + j\left(\frac{f}{2\pi}\right)\gamma} \tag{12}$$

where  $f_R$  is the resonance frequency and  $\gamma$  is the damping parameter of a laser.

The above equation has been used to plot the relative response versus frequency for the designed 420nm laser both with and without oxide confinement layer as shown in Figure 10.

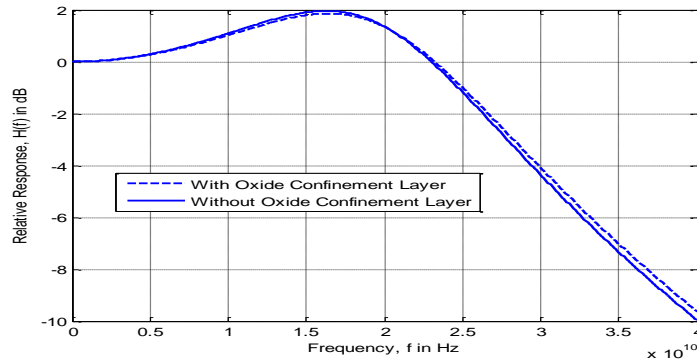


Fig. 10: Plots of Relative Response versus Frequency for the Designed 420nm laser both with and without oxide confinement layer.

From Figure 10 it has been found that the resonance frequency is 16.2 GHz and modulation bandwidth is 28.2GHz at 130mA injection current for the designed laser without oxide confinement layer. It is possible to obtain the same value of resonance frequency and modulation bandwidth, that is, 16.2GHz and 28.2GHz respectively at an injection current of 45mA only for the designed laser with oxide confinement layer.

#### 4 CONCLUSIONS

The difference between the performance analysis of a 420nm designed laser with oxide confinement layer and without oxide confinement layer has been presented in this work. For both the designed laser with and without oxide confinement layer, the injection current which is around 13 times of the threshold current has been selected. It is possible to achieve the same value for steady state carrier density, steady state photon density and steady state modal gain for different values of injection current- that is, 130mA for the designed laser without oxide confinement layer and 45mA for the designed laser with oxide confinement layer. Particularly, the same value of resonance frequency of 16.2GHz and modulation bandwidth of 28.2GHz has been obtained for the designed laser without oxide confinement layer at an injection current 130mA and the designed laser with oxide confinement layer at an injection current of only 45mA. The maximum output power of the designed oxide confined laser is obtained as 73.4mW. Therefore, the designed laser with oxide confinement layer is preferred as it gives the same performance but at a lower injection current.

#### References

- Aldrige, Simon, & Downs, Anthony J. (2011). *The Group 13 Metals Aluminium, Gallium, Indium and Thallium. Chemical Patterns and Peculiarities*, John Wiley, 623.
- Choi, Rak Jun, Lee, Hyung Jae, Hahn, Yoon-bong, & Cho, Hyung Koun (2004). Structural and optical properties of InGaN/GaN triangular-shape quantum wells with different threading dislocation densities. *Korean Journal of Chemical Engineering*, 21(1), 292-295.
- Eliseev, P. G. (1999). Radiative Processes in InGaN quantum wells. *7th Int. Symp. Nanostructures: Physics & Technology*, 329-335.
- Chen, Liang-Yi, Huang, Ying-Yuan, Chang, Chun-Hsing, Sun, Yu-Hsuan, Cheng, Yun-Wei, Ke, Min-Yung, et al. (2010). High performance InGaN/GaN nanorod light emitting diode arrays fabricated by nanosphere lithography and chemical mechanical polishing process. *Optics Express*, 18(8), 7664-7669.
- Chang, H. J., Hsieh, Y.P., Chen, T. T., Chen, Y. F., Liang, C. -T., Lin, T. Y., et al. (2007). Strong luminescence from strain relaxed InGaN/GaN nanotips for highly efficient light emitters. *Optics Express*, 15(15), 9357-9365.
- Skierbiszewski, C, Perlin, P, Grzegory, I, Wasilewski, Z R, Siekacz, M, Feduniewicz, A, et al. (2005). High power blue-violet InGaN laser diodes grown on bulk GaN substrates by plasma-assisted molecular beam epitaxy. *Semiconductor Science & Technology*, 20(8), 809-813.

- Bergh, Arpad A. (2004). Blue Laser Diode (LD) and Light Emitting Diode (LED) Applications. *Physics Status Solidi (a)*, 201(12), 2740-2754.
- Coldren, L. A., & Corzine, S.W. (1995). *Diode Lasers and Photonic Integrated Circuits*. John Wiley, New York, 1-263.
- Piprek, Joachim, Sink, R. Kehl, Hansen, Monica A., Bowers, John E., & DenBaars, Steve P. (2000). Simulation and Optimization of a 420nm InGaN/GaN Laser Diodes. *Physics and Simulation of Optoelectronic Devices VIII, Proc. of SPIE*, 3944, 1-12.
- Erwin, Grant, Bryce, A. C., & Rue, Richard M. De La (2005). Low threshold oxide-confinement compact edge-emitting semiconductor laser diodes with high reflectivity 1D photonic crystal mirrors. *Lasers and Applications, Proc. of SPIE*, 5958, 59580E-1-7.
- Basak, Rinku (2013). Optimized High Performance Characteristics of a Designed 420nm InGaN/AlGaIn MQW Blue Violet Laser. *American Academic & Scholarly Research Journal*, 5(4), 23-33.
- Alam, Tawsif Alam, Rahim, Md. Abdur, & Basak, Rinku (2013). Design and Performance Analysis of a 635nm Ga<sub>0.5</sub>In<sub>0.5</sub>P/(Al<sub>0.7</sub>Ga<sub>0.3</sub>)<sub>0.5</sub>In<sub>0.5</sub>P Multiple Quantum Well Separate Confinement Heterostructure Red Laser Considering Thermal Limitation. *Trends in Opto-Electro & Optical Communications, STM Journals*, 3(1), 11-17.

**Nadia Afroze** received a Bachelor of Science (B.Sc.) degree in Electrical and Electronic Engineering (EEE) from American International University-Bangladesh (AIUB) in 2010. She is currently studying Masters in EEE at AIUB. She is now with the Department of EEE at AIUB as a Lecturer. She is currently continuing her research in the field of optoelectronic devices.

**Rinku Basak** received B.Sc. Engg. (EEE) degree from Khulna University of Engineering & Technology (KUET) Khulna, Bangladesh in 2004. He received M.Sc. Engg. (EEE) degree from Bangladesh University of Engineering & Technology (BUET) Dhaka, Bangladesh in October 2007. Currently he is working as Head (Graduate Program) of Department of EEE at AIUB. Mr. Basak is a Member of IEEE USA and the Institution of Engineers Bangladesh (IEB). His research interests are on high power and high speed VCSELs, Violet Laser, Blue-Violet Laser, True Blue Laser, and Red Laser.